https://doi.org/10.22226/2410-3535-2021-4-508-513 PACS: 81.20.Vj

Ultrasonic spot welded CP Ti/AA2024/CP Ti alloy joints

A. A. Mukhametgalina†, M. A. Murzinova, A. A. Nazarov

†a.mukhametgalina@mail.ru

Institute for Metals Superplasticity Problems, RAS, Ufa, 450001, Russia

Ultrasonic welding (USW) is a promising technique of solid state joining of similar and dissimilar materials, including aluminum and titanium alloys. Differences in the physical and mechanical properties of the materials to be joined make it difficult to adjust the welding conditions to form high-quality joints. The development of natural aging in aluminum alloys may cause a change in the fracture mode and strength of Al/Ti ultrasonically welded joints. In present study, cryorolled and naturally aged AA2024 alloy sheet and annealed commercially pure titanium sheets were subjected to USW. The pre-treatment provided similar values of the hardness of the initial sheets. To avoid the adhesion of aluminum to the welding tool during welding, the AA2024 alloy sheet was sandwiched between the titanium sheets. Microstructure and properties of the welded joints after natural aging were examined. No cracks, discontinuities, pores were observed near the contact surfaces at magnifications of the microscope up to 1000 times. No diffusional or intermetallic reaction layers were revealed in the welded joints. The microstructure and microhardness of titanium sheets did not change after ultrasonic welding. Recovery/recrystallization development led to a decrease in microhardness of AA2024 alloy sheet. All welded samples fractured along the interface between the AA2024 alloy sheet and the bottom titanium sheet adjacent to the anvil. The average lap shear failure load of the welds was 1612 ± 278 N (shear strength of approximately 57 ±10 MPa).

Keywords: ultrasonic welding; commercially pure titanium; aluminum alloy.

УДК: 621.791.16

Соединения сплавов Ti/AA2024/Ti, полученные точечной ультразвуковой сваркой

Мухаметгалина А. А.†, Мурзинова М. А., Назаров А. А.

Институт проблем сверхпластичности металлов РАН, Уфа, 450001, Россия

Ультразвуковая сварка (УЗС) является перспективным методом соединения однородных и разнородных материалов, в том числе алюминиевых и титановых сплавов. Различия физических и механических свойств соединяемых материалов часто усложняют задачу выбора режимов сварки для получения качественных соединений. Развитие естественного старения в алюминиевых сплавах может вызвать изменение моды разрушения и прочности соединений Al/Ti, полученных ультразвуковой сваркой. В настоящем исследовании криопрокатанный и естественно состаренный лист из сплава АА2024 и отожженные листы из технически чистого титана подвергались УЗС. Предварительная обработка обеспечила близкую твердость исходных листов. Чтобы избежать адгезии алюминия к сварочному инструменту во время сварки, лист из сплава АА2024 был зажат между титановыми листами. Исследованы микроструктура и свойства сварных соединений после естественного старения. При увеличении микроскопа до 1000 раз трещин, несплошностей, пор вблизи контактных поверхностей не наблюдалось. В сварных соединениях не обнаружено диффузионных или интерметаллидных реакционных слоев. Микроструктура и микротвердость титановых листов после ультразвуковой сварки не изменились. Развитие возврата/рекристаллизации привело к снижению микротвердости в листе из сплава АА2024. Все сваренные образцы разрушались вдоль границы раздела между листом из сплава АА2024 и нижним титановым листом, примыкающим к наковальне. Средняя разрушающая нагрузка при испытании на срез составила 1612 ± 278 Н (прочность на сдвиг около 57 ±10 МПа).

Ключевые слова: ультразвуковая сварка, технически чистый титан, алюминиевый сплав.

1. Introduction

Welding of dissimilar materials is gaining more and more importance, as it allows one to obtain structures with a required balance of properties reducing the cost of their production. For example, aluminum alloys are inexpensive and have a low density, while titanium and its alloys exhibit high strength properties and corrosion resistance, and the combination of these materials is widely used in the aviation and automotive industries [1]. Differences in the properties of titanium and aluminum (in the melting point, heat conductivity, coefficient of linear expansion, mutual solubility, etc.) make it difficult to obtain high-quality weld joints. During fusion welding, hard and brittle intermetallic compounds (IMCs) of the Al-Ti system are readily formed at the interface [2 – 4]. In this regard, solid state welding techniques are developed such as diffusion bonding and various types of friction welding. However, their application does not exclude the formation of IMCs in the welds of aluminum and titanium alloys [5, 6]. According to [7], the thickness of the $TiAl_3$ intermetallic layer significantly affects the mechanical properties of Al/Ti joints obtained by friction welding, and the IMC layer thickness cannot exceed the critical value of 5 μm.

One of promising techniques of solid state joining of similar and dissimilar materials, including aluminum and titanium alloys, is ultrasonic welding (USW) [8]. Energy consumption for USW is several times less than for friction stir welding and resistance spot welding [9]. Good quality joints can be obtained in a couple of seconds without any preliminary cleaning of the surfaces to be welded by USW. The strength of USW-processed joints is comparable to that of joints obtained by other welding methods [10]. As a rule, the temperature in the welding zone is far below the melting temperature of the metals to be joined [8]. For example, the temperature reached 365°C during USW of the AA6061 aluminum alloy with commercially pure titanium (CP Ti) [11]. Zhang et al. measured the temperature during welding of Ti6Al4V alloy with AA2139-T8 [12] and A6111 aluminum alloys [13]. They demonstrated that the temperature did not exceed 540°C. These authors did not reveal any intermetallic phases, which were observed in the Al/Ti joints after welding by other methods [2 – 6]. Zhou [11] and Balle [14] also did not find IMCs after USW, and this was associated with the very low welding energy, short time and high activation energy for diffusion in Al-Ti. However, $TiAl_3$ was found in an extremely narrow region after USW of Al5754-O and Ti-6Al-4V sheets with a pure Al interlayer [10]. Authors of the cited paper suggested that during welding the temperature was higher than the melting point of Al, but the temperature was not measured in the study.

USW conditions leading to a satisfactory strength of joints are adjusted experimentally, taking into account the capabilities of the welding system used. For example, joints with comparable strengths were obtained at a compressive pressure of 0.55 MPa and welding energy of 2 kJ in [13] and at a compressive pressure of 15 MPa and welding energy 4 kJ in [11], (the frequency and time of welding were approximately the same). As with other welding techniques, it is difficult to adjust the USW conditions for welding dissimilar materials due to differences in their physical and mechanical properties (thermal conductivity, heat capacity, strength, wear resistance, etc.). Moreover, shear strength and microhardness of USW joints of aluminum and titanium alloys may change as a result of natural aging of aluminum alloys [12,13,15]. Probably, for these reasons, the data on the properties and structure of USW joints of aluminum and titanium alloys often do not coincide and are not reproduced.

The present paper supplements the available information on the structure and properties of joints of titanium and aluminum by studying the USW of commercially pure (CP) Ti and AA2024 alloy. In contrast to the cited studies, the materials to be joined had a similar strength before USW due to a preliminary thermal and deformation treatment.

2. Materials and Methods

Annealed sheet of CP Ti (impurities in wt.% less than: 0.32 Al, 0.1Fe, 0.1Si, 0.05 C, 0.035 N, 0.01H, 0.1O) and cryorolled sheet [16,17] of AA2024 aluminum alloy (Al-4.4 Cu-1.4 Mg-0.7 Mn, wt.%) subjected to natural aging were taken as starting materials. The thickness of both sheets was 0.5 mm. Equiaxed α grains with an average size of 7.4 ± 0.4 μm were observed in the cross section of the starting CP Ti sheet. The initial structure of the cryorolled sheet of AA2024 alloy consisted of about 15 μm thick fibers elongated in the rolling direction with stringers of excess (insoluble) phases [17]. The fine structure of the fibers consists of misoriented cells/subgrains having sizes of 150 – 400 nm and a high dislocation density [17,18]. During natural aging, metastable phases precipitated from the supersaturated aluminum-based solid solution. The described structural conditions provided similar strength characteristics of the welded sheets of CP Ti and AA2024 alloy. For example, the microhardness of both materials was about 1900 MPa [19], and the yield strength was about 300 MPa.

Cards with dimensions of 20 × 40 mm and 13×15 mm were cut from CP Ti and AA2024 alloy sheets, respectively, parallel to the rolling direction. The surfaces to be joined were grinded sequentially using P40 and P220 abrasive papers, then washed with isopropyl alcohol and dried. Cards of AA2024 alloy were placed between CP Ti sheets as shown in Fig. 1a to prevent the adhesion of aluminum to the surface of the anvil and welding tip during USW. USW was carried out on an experimental setup with a vibration frequency of 20 kHz and displacement amplitude of 18 μm. USW was performed for 3 s under clamping force of 3.5 kN (the pressure applied was about 178 MPa, which was approximately 0.6 of the room temperature yield strength of the materials to be joined). The welding tip had the shape of a circle with a diameter of 5 mm. Lateral teeth were made on its surface for its better binding to the surface of the top sheet. A typical view of the welded specimens is shown in Fig. 1b.

The microstructure was investigated in the cross sections of the joints in a plane parallel to the direction of vibrations (Fig. 1b) by scanning electron microscopy on TESCAN MIRA 3 LMH FEG microscope in the backscattered electron (BSE) mode. For structural studies samples were ground and mechanically polished on a colloidal suspension with a grain size of 0.05 μm. Quantitative structural analysis was

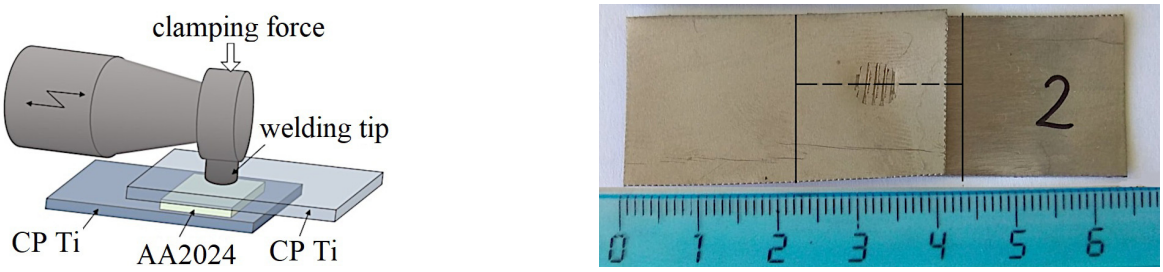

a b

Fig. 1. (Color online) Schematic diagram of the arrangement of sheets and ultrasonic spot welding process (a), and a view of a welded specimen (b); the dashed line indicates the section in which the structure of joint was examined.

performed in accordance with the requirements of ASTM E112-10. The diameter of a grain was accepted as the grain size. The average grain size was estimated by lineal intercept procedure. The average grain diameter $\bar{d}$ was calculated as $\bar{d}=4\bar{l}/\pi$, where $\bar{l}$ is the average intercept length. The statistical error of the average grain size measurement was calculated at a confidence level of 90%. Chemical analysis was performed using a Tescan VEGA 3SBH scanning electron microscope equipped with Oxford energy dispersive X-ray spectroscopy (EDS) system and the AZTech software.

Microhardness measurements were performed via an ITV-1-AM testing instrument with a load on the indenter of 10 g and a dwell time of 10 s. The average value of the microhardness per a point (in each point) was calculated from the results of at least 5 measurements. The standard deviation was taken as the error of the measurement. The welded samples were left for a week at room temperature to allow the natural aging to occur and then subjected to lap tensile shear tests using an Instron 5982 machine with a crosshead speed of 1 mm/min at room temperature. The shear strength of the joints was estimated by dividing the maximum load by the area of the welded tip (19.6 mm^2). The results were averaged over three tests and the standard deviation was taken as the value of the measurement error.

3. Results and discussion

3.1. Macrostructure and microstructure

Fig. 2 shows the macrostructure in cross-section of the joint obtained by the USW. One can see defect-free welds no cracks, discontinuities, pores, etc. are observed at a microscope magnification up to 1000 times (see below Fig. 3). Under the footprint created by the welding tip, the thickness of the AA2024 alloy sheet uniformly decreased by approximately 22%, while titanium sheets were plastically deformed mainly in the areas of the "penetration" of the teeth of the welding tip and the anvil.

Presented in Figs. 3a–c are the microstructures in the central region of the joint and Figs. 3d,e show the microstructures of the sheets outside the zone of interaction with the welding tip, at a distance of 2.5 mm from the perimeter of the weld spot. From a comparison of these figures one can see that the microstructures of the both CP Ti and AA2024 alloy sheets in the central and peripheral regions are identical. It should be noted that the microstructure of the CP Ti does not differ from the initial one, whereas the

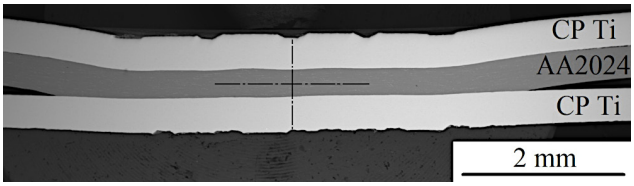

Fig. 2. The macrostructure image in the cross-section of an ultrasonically welded Ti-AA2024-Ti sample.

microstructure of the AA2024 alloy sheet changed. Relatively equiaxed grains/subgrains with a distinct contrast in the BSE images and an average size of 12.4±2.1 μm are revealed in the cross section of the AA2024 alloy sheet (Fig. 3), which were not observed in the initial sheet [17,18]. Evidently, the heating during USW caused the development of recovery and/or recrystallization in the aluminum alloy. The authors of [19] observed a similar microstructure after the annealing of cryorolled AA2024 sheets at 450°C. Under these conditions, the formation of a grain structure is accompanied with a decomposition of the supersaturated solid solution with a precipitation of dispersed particles of the strengthening phases, which are distinguishable only by transmission electron microscopy techniques [19]. It should be noted that heating up to 500°C of pre-annealed titanium does not cause any noticeable structural changes in it [20].

The observed changes in the microstructure are in a satisfactory agreement with the results of microhardness measurements (Fig. 4).

Microhardness of CP Ti before and after USW was 1876±51 MPa. Recovery and/or recrystallization in AA2024 alloy led to a decrease in microhardness from 1860±72 to 1498±40 MPa, which did not differ significantly over the whole thickness of the sheet (Fig. 4a). In contrast to the results of [12,13,15], we did not find significant differences in the microhardness of the AA2024 sheet inside and outside the weld spot (Fig. 4b). We assume that the temperature distribution in the AA2024 sheet sandwiched between the CP Ti sheets was quite uniform, that is, the CP Ti sheets played the role of a "heat insulator", since the thermal conductivity of titanium is 13 and 4 times less than the thermal conductivity of aluminum and steel (anvil and tip material) respectively.

3.2. EDS analysis

To detect and estimate the width of a layer with a changed chemical composition near the contact surfaces of the sheets

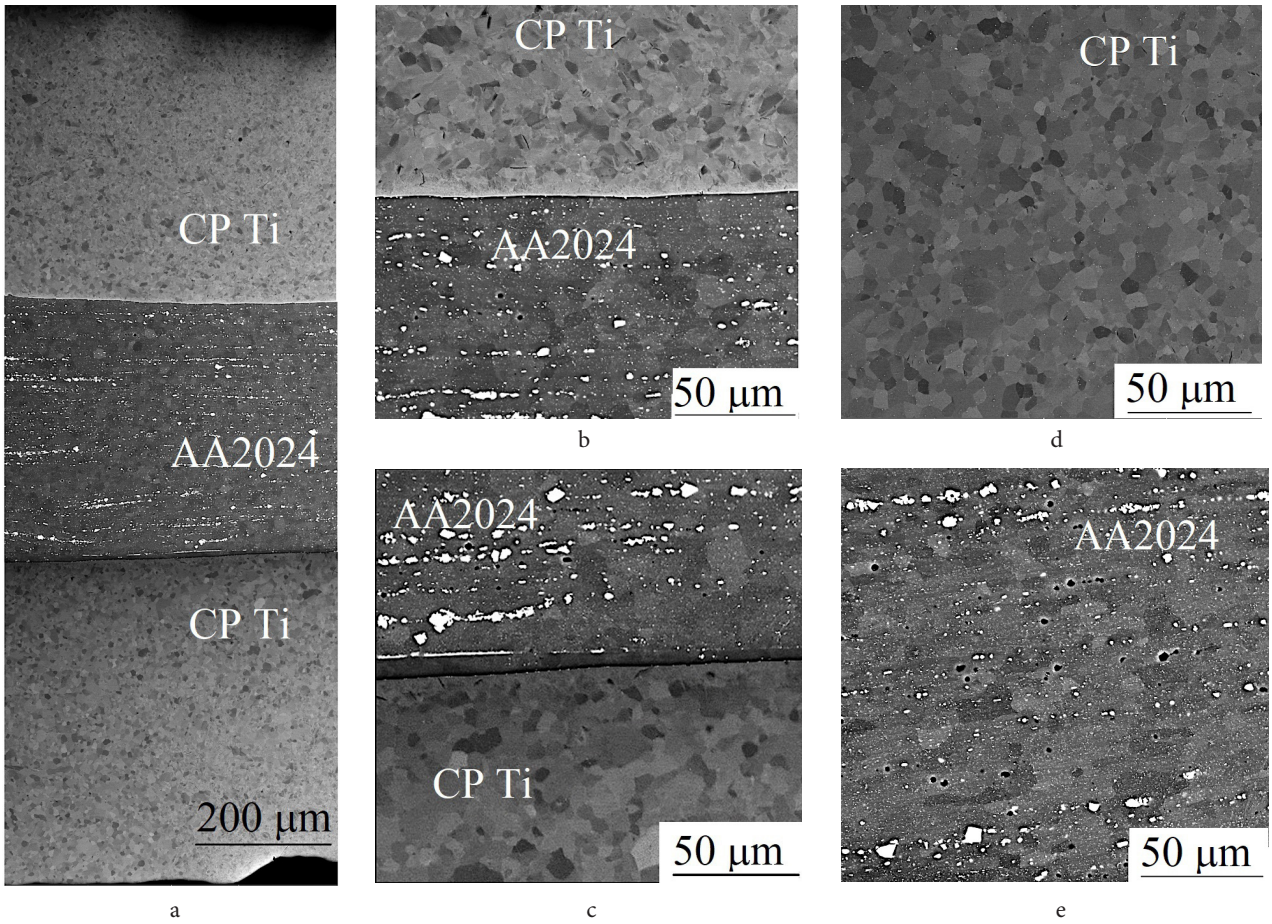

Fig. 3. BSE images of the microstructure in the central region of the welded joint (a), top weld (b), bottom weld (c); and the microstructure of the sheets at a distance of 2.5 mm from the perimeter of the welded spot: CP Ti (d), AA2024 alloy (e).

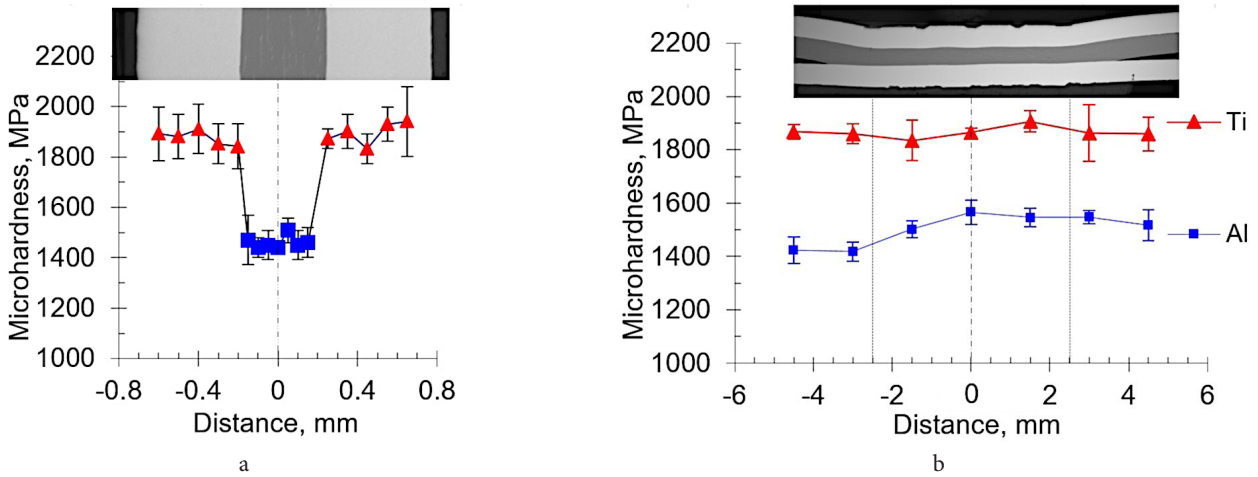

Fig. 4. (Color online) Microhardness of CP Ti and AA2024 alloy sheets after USW in vertical (a) and horizontal (b) directions.

to be joined, an energy-dispersive analysis was carried out along the lines intersecting the contact planes. Fig. 5 shows typical profiles of Ti and Al distribution in different zones of the welded joints. In all cases, the transition zone between the sheets has a width of about 4 μm, which is comparable to the size of the region of interaction of the electron probe with metals. For this reason, it is impossible to determine reliably the width of the zone with changed chemical composition, as well as the presence or absence of particles of intermetallic phases ($TiAl_3$, TiAl and Ti_3Al) if theirs sizes are less than 4 μm. EDS results for the top and bottom welds, as well as for the center and periphery of the joint, were similar. The obtained result is consistent with the data of [12,13,15], in which IMCs were not detected not only by EDS analysis, but also by transmission electron microscopy.

3.3. Mechanical Properties

A typical view of the sample after mechanical lap shear tests is shown in Fig. 6. The average value of the failure load was 1612 ± 278 N. For comparison with the literature data, a more convenient characteristic of the shear strength of the joint

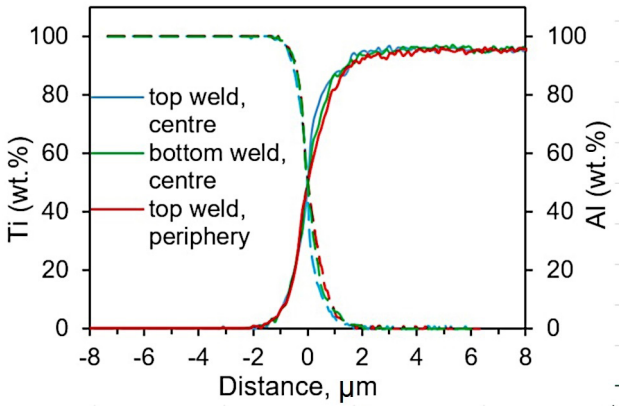

Fig. 5. (Color online) Distributions of Ti and Al along lines perpendicular to the top and bottom welds planes in the central and peripheral regions of the sample.

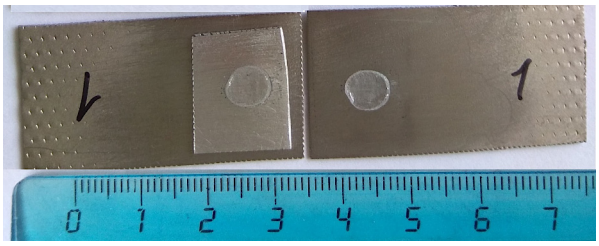

Fig. 6. (Color online) A typical view of the sample after lap tensile shear test.

is the failure load per unit area of the welding tip. The shear strength values of dissimilar Al/Ti ultrasonically welded joints published in a number of articles are listed in Table 1.

It can be seen that the shear strength of the joints obtained in this work is close to shear strength presented in several references [11–14]. The authors of [10,15] achieved much higher strength, but in these studies, a foil or pure Al powder was placed between the sheets of titanium and aluminum alloys. It should be noted that the lap shear test results obtained in this work characterize the strength of the "weak" bottom weld, since the failure of all samples occurred between the AA2024 alloy sheet and the bottom CP Ti sheet adjacent to the anvil. Obviously, the joint between the top CP Ti sheet and the AA2024 alloy is stronger. Two reasons to explain this difference can be assumed. First, the efficiency of the transmission of vibrations from the welding tip to the bottom contact surface decreases due to the loss of mechanical energy in the top weld joint owing to the internal friction and the resulting heat generation [21]. Second, after welding always there is a specific deformation of the top two sheets, as one can see in Fig. 2. This deformation results in a sharper stress concentrator along the perimeter of the bottom weld as compared to the one of the upper weld during testing. Both reasons might result in a lower strength of the lower weld joint. Probably, the strength of this lower joint can be increased by: 1) reducing the thickness of the AA2024 sheet, which will reduce the loss of mechanical energy during welding; 2) changing the shape of the welding tip and reducing the clamping force, which will change the distribution of stresses along the perimeter of this joint.

Table 1. Shear strength of dissimilar Al/Ti ultrasonic welds.

Welded alloys	Failure load (N)/A (mm^2), MPa	Ref.
AA2024/CP Ti	57±10	This study
AA2139-T8/TiAl6V4	67.5	[12]
AA6061/CP Ti	51.3	[11]
AA6111/TiAl6V4	57.4	[13]
AA7075/TiAl6V4	56.2	[14]
Al6061/pure Al powder/ Ti6Al4V	106	[15]
Al5754–O/pure Al/Ti6Al4V	206	[10]

4. Conclusion remarks

Ultrasonic welding was used to obtain joints of CP Ti and AA2024 alloy sheets. Before welding, these sheets exhibited similar values of hardness that was achieved by preliminary deformation and heat treatment. To avoid the adhesion of aluminum to the welding tool during welding, the AA2024 alloy sheet was sandwiched between the CP Ti sheets. This arrangement of the sheets ensured a more uniform temperature distribution in the joined sheets, as follows from microstructural observations and microhardness measurements.

Cracks, discontinuities, pores in welds were not observed at magnifications of the microscope up to 1000 times. No intermetallic phases were found near both contact surfaces.

Failure of all samples occurred along the bottom interface between of AA2024 alloy sheet and CP Ti sheet. The average lap shear failure load was 1612 ± 278 N that corresponded to lap shear strength of 57 ±10 MPa. This value is close to the strength of Al/Ti joints given in [11–14].

Acknowledgements. The present work was accomplished in terms of the state assignment of the Institute for Metals Superplasticity Problems of the Russian Academy of Sciences financed by the Ministry of Science and Higher Education of Russia. Electron microscopic studies and mechanical tests were carried out on the facilities of shared services center of IMSP RAS "Structural and Physical-Mechanical Studies of Materials". The authors would also like to thank S. V. Krymskiy, E. V. Avtokratova and O. Sh. Sitdikov for the supply AA2024 alloy cryorolled sheet and helpful discussions on the microstructure evolution in this material.

References

1. K. H. Rendigs. Mater. Sci. Forum. 242, 11 (1997). Crossref
2. K. Liu, Y. Li, S. Wei, J. Wang. Mater. Manuf. Process. 29 (8), 969 (2014). Crossref
3. I. Tomashchuk, P. Sallamand, E. Cicala, P. Peyre, D. Grevey. J. Mater. Process Technol. 217, 96 (2015). Crossref
4. S. Chen, L. Li, Y. Chen, J. Huang. J. Alloys Compd. 509 (3), 891 (2011). Crossref
5. R. Jiangwei, L. Yajiang, F. Tao. Mater. Lett. 56 (5), 647 (2002). Crossref
6. M. Aonuma, K. Nakata. Mater. Trans. 52 (5), 948 (2011). Crossref
7. Y. C. Kim, A. Fuji. Sci. Technol. Weld. Join. 7 (3), 149 (2002). Crossref

8. M. P. Matheny, K. F. Graff. In: Power Ultrasonics (Ed. by J. A. Gallego-Juárez, K. F. Graff). Woodhead Publishing, UK (2015) pp. 259 – 293. Crossref
9. D. Bakavos, P. B. Prangnell. Mater. Sci. Eng. A. 527 (23), 6320 (2010). Crossref
10. S. Q. Wang, V. K. Patel, S. D. Bhole, G. D. Wen, D. L. Chen. Mat. Des. 78, 33 (2015). Crossref
11. L. Zhou, J. Min, W. X. He, Y. X. Huang, X. G. Song. J. Manuf. Process. 33, 64 (2018). Crossref
12. C. Q. Zhang, J. D. Robson, P. B. Prangnell. J. Mater. Proc. Technol. 231, 382 (2016). Crossref
13. C. Q. Zhang, J. D. Robson, O. Ciuca, P. B. Prangnell. Mater. Charact. 97, 83 (2014). Crossref
14. F. Balle, J. Magin. Phys. Procedia. 70, 846 (2015). Crossref
15. H. M. Zhang, Y. J. Chao, Z. Luo. Sci. Technol. Weld. Join. 22 (1), 79 (2017). Crossref
16. M. V. Markushev, E. V. Avtokratova, I. Ya. Kazakulov, S. V. Krymskiy, M. Yu. Mochalova, M. Yu. Murashkin, O. Sh. Sitdikov. Deformation and Failure of Mater. 4, 36 (2010). (in Russian) [М. В. Маркушев, Е. В. Автократова, И. Я. Казакулов, С. В. Крымский, М. Ю. Мочалова, М. Ю. Мурашкин, О. Ш. Ситдиков. Деформация и разрушение материалов. 4, 36 (2010).]
17. E. V. Avtokratova, S. V. Krymsky, M. V. Markushev, O. Sh. Sitdikov. Letters on Materials. 1 (2), 92 (2011). (in Russian) [Е. В. Автократова, С. В. Крымский, М. В. Маркушев, О. Ш. Ситдиков. Письма о материалах. 1 (2), 92 (2011).] Crossref
18. S. V. Krymskiy, E. V. Avtokratova, O. S. Sitdikov, M. V. Markushev, A. V. Mikhaylovskaya. The Physics of Metals and Metallography. 116 (7), 676 (2015). Crossref
19. R. R. Ilyasov, E. V. Avtokratova, A. D. Kotov, S. V. Krymsky, M. V. Markushev, A. V. Mikhailovskaya, O. Sh. Sitdikov. Tambov University Reports. 21 (3), 1033 (2016). (in Russian) [Р. Р. Ильясов, Е. В. Автократова, А. Д. Котов, С. В. Крымский, М. В. Маркушев, А. В. Михайловская, О. Ш. Ситдиков. Вестник Тамбовского университета. 21 (3), 1033 (2016).] Crossref
20. G. Lütjering, J. C. Williams. Titanium, 2nd edition. Berlin, Heidelberg, New York, Springer (2007).
21. E. de Vries. Mechanics and mechanisms of ultrasonic metal welding: Ph.D. dissertation. The Ohio State University, Columbus, OH (2004).